Semiconductors, 2022, Vol. 56, No. 9

Self-powered photo diodes based on Ga_2O_3/n-GaAs structures

© V.M. Kalygina, O.S. Kiselyeva, B.O. Kushnarev, V.L. Oleinik, Yu.S. Petrova, A.V. Tsymbalov

Tomsk State University,
634050 Tomsk, Russia

E-mail: kalygina@ngs.ru

Received April 18, 2022
Revised July 28, 2022
Accepted July 28, 2022

The electrical and photovoltaic characteristics of the Ga_2O_3/n-GaAs structures have been studied. A gallium oxide film was obtained by HF magnetron sputtering on n-GaAs epitaxial layers with concentration of $N_d = 9.5 \cdot 10^{14}\,\text{cm}^{-3}$. The thickness of the oxide film was 120 nm. Measurements at a frequency of 10^6 Hz have shown that the capacitance-voltage and conductance-voltage dependences are described by curves characteristic of metal-insulator-semiconductor structures and exhibit low sensitivity to radiation with $\lambda = 254$ nm. When operating on a constant signal, the samples exhibit the properties of a photodiode and are able to work offline. The photoelectric characteristics of the detectors during continuous exposure to radiation with $\lambda = 254$ nm are determined by the high density of traps at the Ga_2O_3/GaAs interface and in the oxide film.

Keywords: MIS-structures, capacitance-voltage characteristics, volt-siemens characteristics, photocurrent, trap density.

DOI: 10.21883/SC.2022.09.54139.9868

1. Introduction

The fabrication of devices capable of self-powered operation is one of the promising directions in design of short-wave radiation detectors. Self-powered photodetectors have a number of advantages over other devices based on wide-gap materials sensitive to ultraviolet radiation. Such photodetectors have a simple design and, most crucially, provide for direct integration with the metal–insulator–semiconductor (MIS) fabrication technology [1]. A considerable number of studies focused on the electric and photovoltaic characteristics of metal–Ga_2O_3–semiconductor structures have already been published. Organic and inorganic materials were used in these studies as semiconducting substrates [2–9]. The electric and optical parameters of such devices are governed by the choice of a semiconductor, the technique and conditions of fabrication of a Ga_2O_3 film, and the specifics of oxide film processing after deposition onto a semiconducting substrate. In the present study, we report the results of examination of electric and photovoltaic characteristics of structures fabricated by HF magnetron sputtering of a gallium oxide film onto epitaxial n-GaAs layers.

2. Experimental procedure

Epitaxial n-GaAs layers with concentration $N_d = 9.5 \cdot 10^{14}\,\text{cm}^{-3}$ were used as a substrate. These layers with a thickness of $12\,\mu$m were grown on single-crystal GaAs(100) wafers. The thickness of a buffer n^+-type layer was $4.9\,\mu$m. Following the deposition of an oxide film, Ga_2O_3/n-GaAs structures were annealed in argon for 30 min at a temperature of 900°C.

The phase composition of films was determined by X-ray diffraction analysis (XDA) performed using a Lab-X XRD 6000 (Shimadzu) diffractometer. An X-ray tube with a copper anode was used to examine the atomic structure. The operating wavelength was 1.54 nm. Computer processing of the obtained data was performed in OriginPro8.

Platinum contacts were deposited onto the Ga_2O_3 surface and the back side of a semiconductor substrate to measure the electric characteristics. The contact to a semiconductor was sputtered in the form of a solid metal film, while the contact to gallium oxide was formed by sputtering metal through masks 1 mm in diameter. The area of the electrode to Ga_2O_3 (gate) was $1.04 \cdot 10^{-2}\,\text{cm}^2$.

Dark current–voltage characteristics (CVCs) and CVCs under ultraviolet irradiation were examined at room temperature using a Keithley 2611B sourcemeter. A VL-6 krypton–fluorine lamp with a 254-nm filter served as the source of UV radiation. The distance between the lamp and the sample was 1 cm, and the incident radiation intensity was $0.78\,\text{mW/cm}^2$.

Capacitance–voltage and conductance–voltage characteristics of the obtained samples were measured at a frequency of 1 MHz. An E7-12 LCR meter and a specially designed attachment, which allows one to measure automatically capacitance–voltage ($C-U$) and conductance–voltage ($G-U$) characteristics in a single cycle, were used for this purpose.

3. Experimental data and discussion

Figure 1 presents the XDA results for a gallium oxide film prepared by HF magnetron sputtering on a GaAs substrate after annealing in argon for 30 min at 900°C.

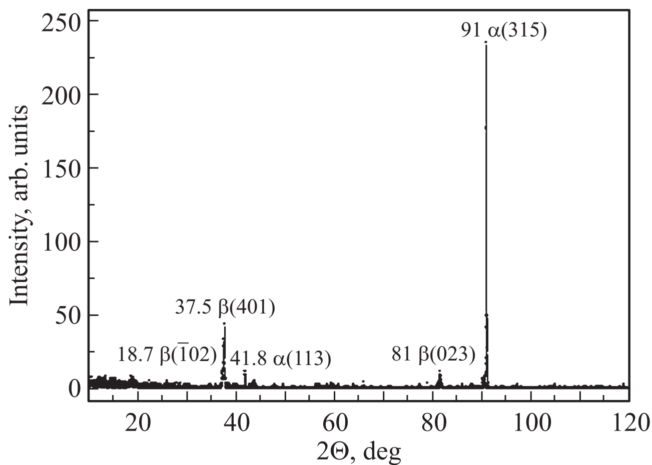

Figure 1. XDA data for a gallium oxide film after annealing in Ar at 900°C.

Crystallites of the β phase oriented in the [$\bar{1}$02], [401], and [023] directions are present in the Ga_2O_3 film.

The $C-U$ and $G-U$ dependences of the samples (Fig. 2,a) are characterized by curves typical of metal−insulator−semiconductor structures. The oxide film thickness calculated using the formula for a plane capacitor and the insulator capacitance value in enrichment ($C_d = 740\,\text{pF}$) is 124 nm.

The calculation of carrier concentration in the semiconductor material with the use of the capacitance–voltage characteristic in depletion (Fig. 3) yielded $N_d = 1.5 \cdot 10^{15}\,\text{cm}^{-3}$. With the experimental error taken into account, this value agrees fairly well with the initial electron concentration in the epitaxial film.

Thus, in contrast to the Ga_2O_3 film fabrication by electrochemical anodizing [10], HF magnetron sputtering of a gallium oxide film does not alter the initial electron concentration in GaAs.

When UV radiation is switched on, only a slight increase in conductance G in depletion is observed (Fig. 4); the capacitive properties of the structure remain essentially unchanged.

Dark current–voltage characteristics of the samples (I_D) are nonlinear and are shaped by the sign and magnitude of the gate voltage (Fig. 5). The rectification factor at a voltage of $\pm 4\,\text{V}$ is 10^3.

The forward current decreases under UV irradiation, while the backward current increases. The effect of radiation with $\lambda = 254\,\text{nm}$ is the most pronounced at low negative and positive sample voltages in the vicinity of $U \approx 0\,\text{V}$. Such structures feature a voltaic effect and are commonly referred to as self-powered photo diodes. Open-circuit voltage U_{oc} for the majority of samples examined in the present study is $(0.40-0.43)\,\text{V}$, and short-circuit current I_{sc} is $(4-10) \cdot 10^{-7}\,\text{A}$.

Figure 6 characterizes the effect of continuous UV irradiation on the CVCs of samples in finer detail (curves $I_{L1}-I_{L5}$). The greatest variation of forward and backward currents under continuous UV irradiation is observed at the first sampling of the detector (I_{L1}); in subsequent CVC measurements, the variations become less pronounced (Fig. 6, curves $I_{L2}-I_{L5}$).

In common with many UV detectors based on gallium oxide films, the M/Ga_2O_3/n-GaAs structures studied here feature residual currents, which are denoted as I_{D1} in Fig. 6.

The studied M/Ga_2O_3/n-GaAs structures operate similarly to photodiodes in the voltaic regime. The backward current increases by more than 2 orders of magnitude under irradiation with $\lambda = 254\,\text{nm}$ and voltage $U = -0.012\,\text{V}$; this provides an opportunity to use such structures as UV radiation detectors in the 200−280 nm wavelength range. At near-zero voltages, the persistent conductivity has almost no effect on the temporal characteristics of detectors. Figure 7 shows the temporal variation of the diode conductivity with UV irradiation switched on and off under a voltage of 0.005 V.

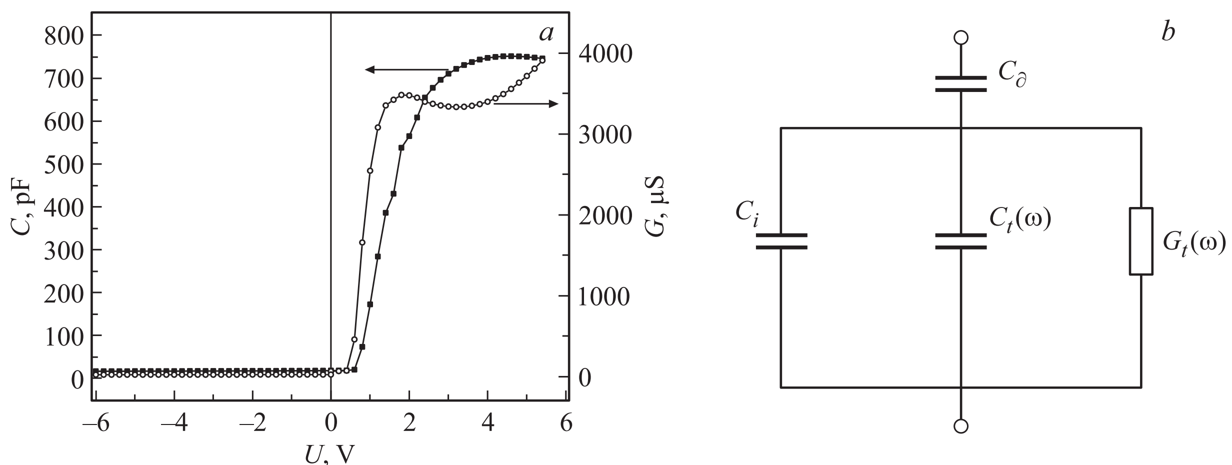

Figure 2. Capacitance–voltage and conductance–voltage characteristics of the Ga_2O_3/n-GaAs structure (a); equivalent circuit used to calculate the density of states at the Ga_2O_3/GaAs interface (b).

Rise τ_r and fall τ_f times determined at the level of 0.9 and 0.1 respectively, do not exceed $1-2$ s; 0.1 fall time τ_f is $(1-2)$ s (Fig. 7, *b*), which is better than the temporal parameters of UV detectors based on barrier structures with interdigital electrodes [11].

The photocurrent reduction after repeated sampling of structures under continuous UV irradiation (Fig. 6) is attributable to the fact that trap centers are involved in shaping the response. The photocurrent is produced both by the transition of electrons from the valence band to the conduction band and the ejection of carriers from trap centers. Traps are localized in the band gap of the oxide film [12–14] and at the Ga_2O_3/GaAs interface. Owing to a significant mismatch between the parameters of a monoclinic Ga_2O_3 lattice and a sphalerite GaAs lattice, a high density of surface states at the interface is expected. The contribution of traps to the photocurrent response decreases in the process of their depletion, and the photocurrent becomes stabilized (Fig. 6, curves $I_{L2}-I_{L5}$).

Trap center density N_t at the Ga_2O_3/GaAs interface was estimated using the capacitance–voltage and conductance–voltage characteristics of MIS structures measured by the bridge method with parallel connection of capacitance (C) and conductance (G). In order to do that, one needs to convert the obtained C and G values using formulae (1)–(3) in

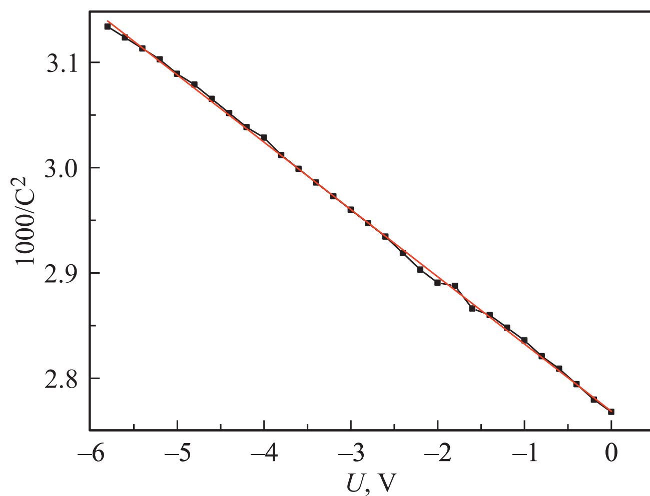

Figure 3. Voltage dependence of the reciprocal capacitance squared.

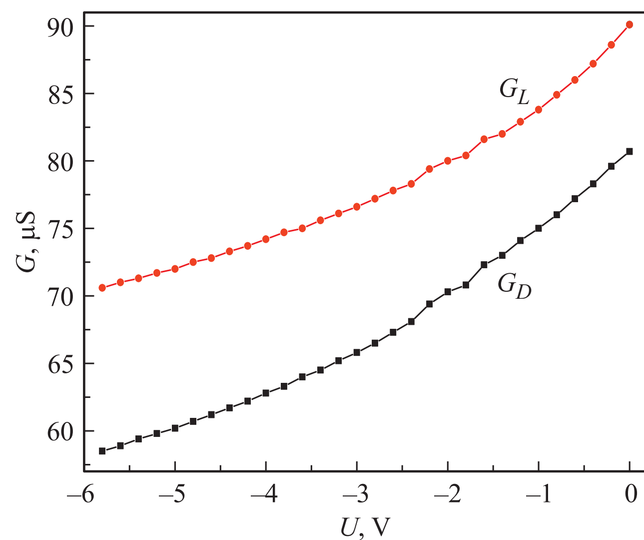

Figure 4. Dark (G_D) conductance–voltage characteristic of the M/Ga_2O_3/n-GaAs structure in depletion and $G-U$ dependence measured under irradiation with $\lambda = 254$ nm (G_L).

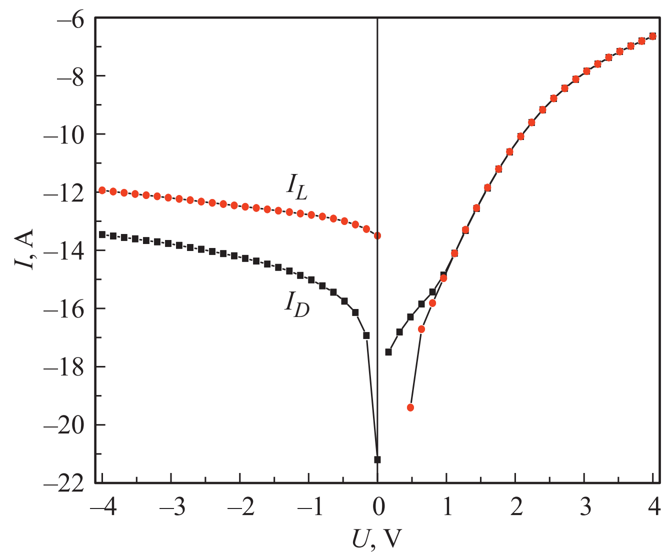

Figure 5. Dark (I_D) current–voltage characteristic of the sample under positive and negative gate voltages and $I-U$ dependence measured under irradiation with $\lambda = 254$ nm (I_L).

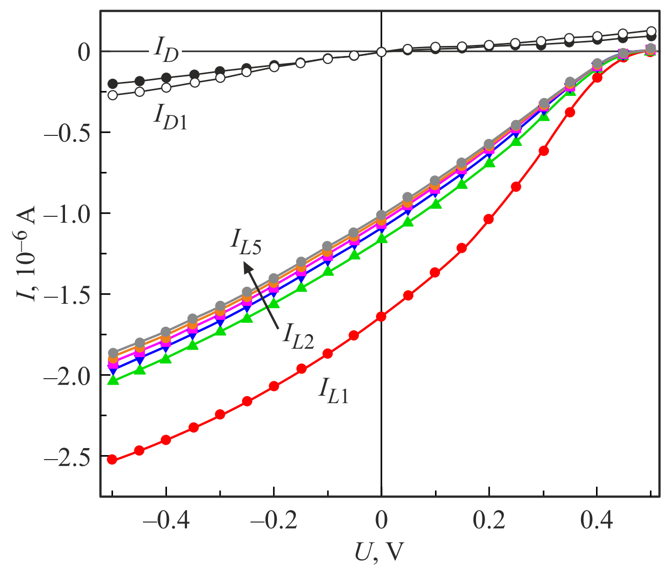

Figure 6. Dark (I_D) current–voltage characteristics of the sample under positive and negative gate voltages and $I-U$ dependences measured under irradiation with $\lambda = 254$ nm ($I_{L1}-I_{L5}$).

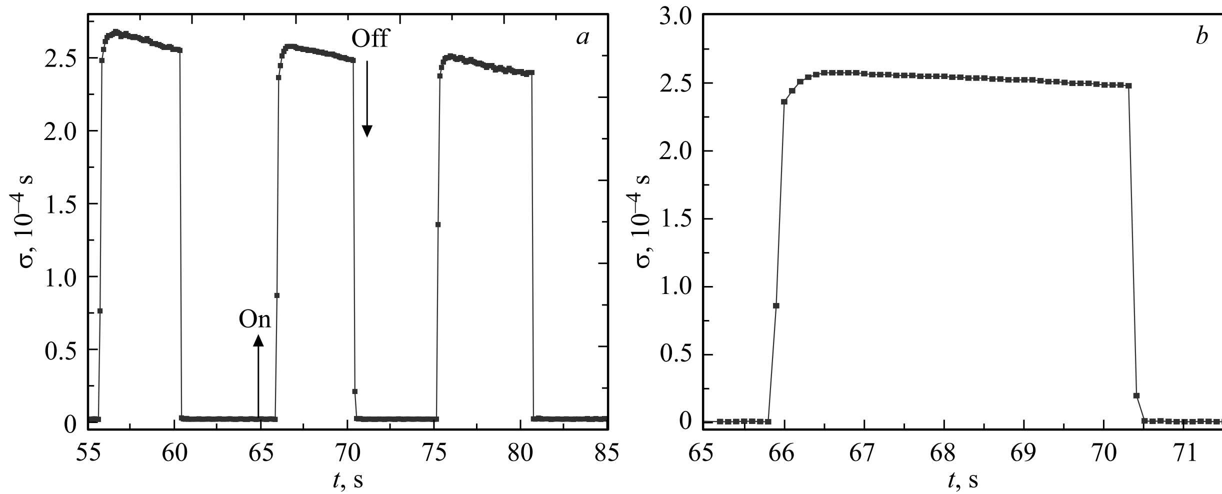

Figure 7. Temporal variation of the conductivity of the M/Ga_2O_3/*n*-GaAs structure with UV irradiation with $\lambda = 254$ nm switched on and off (*a*); close up of an individual pulse (*b*). $U = 0.005$ V.

accordance with the equivalent circuit in Fig. 2, *b* and derive dependences $C_{sc}(\omega)$ and $G_t(\omega)/\omega$ [15]:

$$C_{sc}(\omega) = \frac{\omega^2 C_\partial^2 C - C_\partial(G^2 + \omega^2 C^2)}{G^2 + \omega^2 (C_\partial - C)^2}, \quad (1)$$

$$\frac{G_t(\omega)}{\omega} = \frac{\omega C_\partial^2 G}{G^2 + \omega^2 (C_\partial - C)^2}, \quad (2)$$

$$C_{sc}(\omega) = C_i + C_t(\omega). \quad (3)$$

Here, C_{sc} is the capacitance of the spatial charge region; C_∂ is the insulator capacitance; C_t and G_t are the differential capacitance and conductance attributable to the recharge of surface states with their energy levels being coincident with the Fermi level at the semiconductor surface (F_s); and C_i is the inversion layer capacitance. The following formula may be used to calculate the inversion layer capacitance [15]:

$$C_i = S\left(\frac{\varepsilon\varepsilon_0 e N_d}{2|\varphi_s|}\right)^{1/2}, \quad (4)$$

where S is the area of the electrode to the insulator material, ε is the semiconductor permittivity, ε_0 is the permittivity of vacuum, and φ_s is the surface potential. In experiments, capacitance C_i is determined by finding the minimum measured capacitance value ($C_{\min}$) in capacitance-voltage characteristics under high negative bias voltages at the MIS structure

$$\frac{1}{C_{\min}} = \frac{1}{C_\partial} + \frac{1}{C_i}. \quad (5)$$

The voltage dependence of $G_t(\omega)/\omega$ is characterized by a curve with a maximum at the same voltage that corresponds to the maximum of curve $G(U)$ in Fig. 2, *a*. Using the data obtained in accordance with (2) and formula (6) [15]

$$\left(\frac{G_t}{\omega}\right)_{\max} \approx 0.4 e^2 N_t(F_s), \quad (6)$$

we found energy trap density $N_t = 03.2 \cdot 10^{13}\,\mathrm{eV^{-1}} \cdot \mathrm{cm^{-2}}$. This N_t value characterizes the density of states only at the Ga_2O_3/GaAs interface and, as was noted above, is attributable to the mismatch of lattice parameters of gallium oxide and gallium arsenide. The variation of photocurrent of Ga_2O_3/*n*-GaAs structures under continuous irradiation with $\lambda = 254$ nm is governed by traps both at the interface and in the bulk of the oxide film.

4. Conclusion

The electric and photovoltaic characteristics of Ga_2O_3/GaAs structures fabricated by HF magnetron sputtering of a gallium oxide film onto epitaxial *n*-GaAs layers with concentration $N_d = 9.5 \cdot 10^{14}\,\mathrm{cm^{-3}}$ were examined. The oxide film thickness was 120 nm. The capacitance–voltage and conductance–voltage characteristics of the samples are characterized by curves typical of metal–insulator–semiconductor structures. Ga_2O_3/*n*-GaAs structures were found to be weakly sensitive to radiation with $\lambda = 254$ nm in measurements at a frequency of 10^6 Hz. In continuous signal operation, the samples exhibit photodiode properties and the capacity for self-powered operation. The photovoltaic parameters of detectors under continuous irradiation with $\lambda = 254$ nm are defined by a high density of traps at the Ga_2O_3/GaAs interface and in the bulk of the oxide film.

Conflict of interest

The authors declare that they have no conflict of interest.

References

[1] J. Bae, Ji-H.Park, D.-W.Jeon, J. Kim. APL Mater., **9**, 101108 (2021).

[2] A. Atilgan, A. Yildiz, U. Harmanci, M.T. Gulluoglu, K. Salimi. Mater. Today Commun., **24**, 101105 (2020).

[3] Y. Cui, S. Zhang, Q. Shi, S. Hao, A. Bian, X. Xie, Z. Liu. Phys. Scr., **96**, 125844 (2021).
[4] S. Li, Z. Yan, Z. Liu, J. Chen, Y. Zhi, D. Guo, P. Li, Z. Wu, W. Tang. J. Mater. Chem. C, **8**, 1292 (2020).
[5] Z. Yan, S. Li, J. Yue, X. Ji, Z. Liu, Y. Yang, P. Li, Z. Wu, Y. Guo, W. Tang. J. Mater. Chem. C, **9**, 14788 (2021).
[6] Z. Yan, S. Li, J. Yue, X. Ji, Z. Liu, Y. Yang, P. Li, Z. Wu, Y. Guo, W. Tang. ACS Appl. Mater. & Interfaces, **13**, 57619 (2021).
[7] D. You, C. Xu, J. Zhao, W. Zhang, F. Qin, J. Chen, Z. Shi. J. Mater. Chem. C, **7**, 3056 (2019).
[8] H. Lin, A. Jiang, S. Xing, L. Li, W. Cheng, J. Li, W. Miao, X. Zhou, L. Tian. Nanomaterials, **12**, 910 (2022).
[9] B.R. Tak, M.M. Yang, Y.H. Lai, Y.H. Chu, M.A.R. Singh. Scientific Rep., 10:16098 (2020).
[10] V.M. Kalygina, V.V. Vishnikina, A.N. Zarubin, Yu.S. Petrova, M.S. Skakunov, O.P. Tolbanov, A.V. Tyazhev, T.M. Yaskevich. Russ. Phys. J., **56**, 984 (2014).
[11] V.M. Kalygina, A.V. Tsymbalov, A.V. Almaeva, Yu.S. Petrova. Semiconductors, **55**, 341 (2021).
[12] B.R. Tak, M. Yang, M. Alexe, R. Singh. Crystals, **11**, 1046 (2021).
[13] Y.K. Frodason, K.M. Johansen, L. Vines, J.B. Varley. Appl. Phys., **127**, 075701 (2020). doi: 10.1063/1.5140742
[14] Y.J. Zhang, J. Shi, D.-C. Qi, L. Chen, H.L. Zhang. APL Mater., **8**, 020906 (2020).
[15] V.I. Gaman, N.N. Ivanova, V.M. Kalygina, E.B. Sudakova. Russ. Phys. J., **35**, 1078 (1992).